Journal of Statistical Physics, Vol. 38, Nos. 5/6, 1985

Noisy Precursors of Nonlinear Instabilities

Kurt Wiesenfeld[1]

Received May 1, 1984; revised August 21, 1984

This paper studies the effect of external noise on systems displaying nonlinear instabilities of periodic orbits. Each class of instability is found to have its own characteristic signature, as displayed by the power spectrum. Results are derived for each of the codimension-one instabilities familiar from bifurcation theory.

KEY WORDS: Noise; power spectra; bifurcations; Floquet theory.

1. INTRODUCTION

This paper explores the effect of noise on systems displaying periodic behavior when they are close to a dynamical instability. The very notion of instability implies that small fluctuations grow with time—a system which is "close" to being unstable can be expected to be extremely sensitive to external perturbations. These ideas are very familiar from studies of critical phenomena in statistical mechanics, as well as from stability analyses of nonlinear dynamical systems.

Broadly speaking, we can distinguish between various kinds of dynamical behavior that can become unstable: time-independent solutions, corresponding to fixed points of differential equations; regular time dependence, such as periodic or quasiperiodic oscillations; and chaotic behavior, which has received the lion's share of the recent attention directed toward nonlinear dynamical systems. The present work focuses on the instabilities of periodic orbits, and in particular on the effects of external noise on the observed power spectrum for a system near an instability. We further restrict attention to the various classes of codimension-one bifurcations; that is, the typical instabilities encountered as a single parameter is varied.

Often, periodic orbits are studied by considering a Poincaré return

[1] Department of Physics, University of California, Berkeley, California 94720. Present address: Department of Physics, University of California, Santa Cruz, California 95064.

map associated with that orbit. The advantage of this approach is that it turns a nonlocal stability analysis of a continuous flow into a local stability analysis of a discrete map of one fewer dimension. The drawback is that, in practice, it is extremely difficult to analytically construct the appropriate mapping from the differential equation.

Related to this difficulty is the problem of modeling the external noise. Usually, one has a better physical feel for the differential equation, so the model of fluctuations is better motivated by introducing a random element to the differential equation, rather than to the reduced discrete mapping. Consequently, this paper does not make the reduction to discrete maps, although (see Fig. 2) the basic ideas may be usefully pictured in terms of such maps.

The original motivation for the present work came from measurements performed on a nonlinear circuit.[1] The task there was to determine the precise value of bias current where the onset of a period doubling instability occurred. Far from being interested in the effects of noise on the system, we wanted (as is the usual case in experimental physics) to reduce the background noise as much as possible. A typical sequence of power spectra is sketched qualitatively in Fig. 1—the signal for period doubling is the appearance of a small spike at one-half the fundamental frequency ω. The instability has certainly occurred by the time one reaches Fig. 1e; unfortunately, the substantial broad-band noise rise centered at $\omega/2$ in Fig. 1d makes precise determination of the onset of the instability all but impossible.

The simple picture developed in this paper explains the major features of Fig. 1; however, the theory developed also implies a generality that should extend to all other codimension-one dynamical instabilities, regardless of the physics behind the governing differential equations. In fact, the basic predictions of the theory have been tested by, and agree with, experiments on driven p–n junctions.[2]

To put the present work into context, we call attention to a sample of other recent investigations of the effect of noise on the instabilities of periodic dynamical systems.[3–12] Usually, these works take as starting point a discrete mapping,[3,5–12] rather than a continuous flow,[4] subject to random noise with the focus on either the asymptotic probability density or the power spectrum. By and large, the emphasis has been on the *scaling laws* for the bifurcations of dynamical systems leading to chaos. For example, one well-studied problem concerns the level of random noise required to obscure the remainder of the cascade of period doubling bifurcations beyond some given 2^N-periodic oscillation. The scaling of this level as $N \to \infty$ has been determined theoretically in a variety of ways for the universality class represented by the logistic map,[3–6] and agrees with

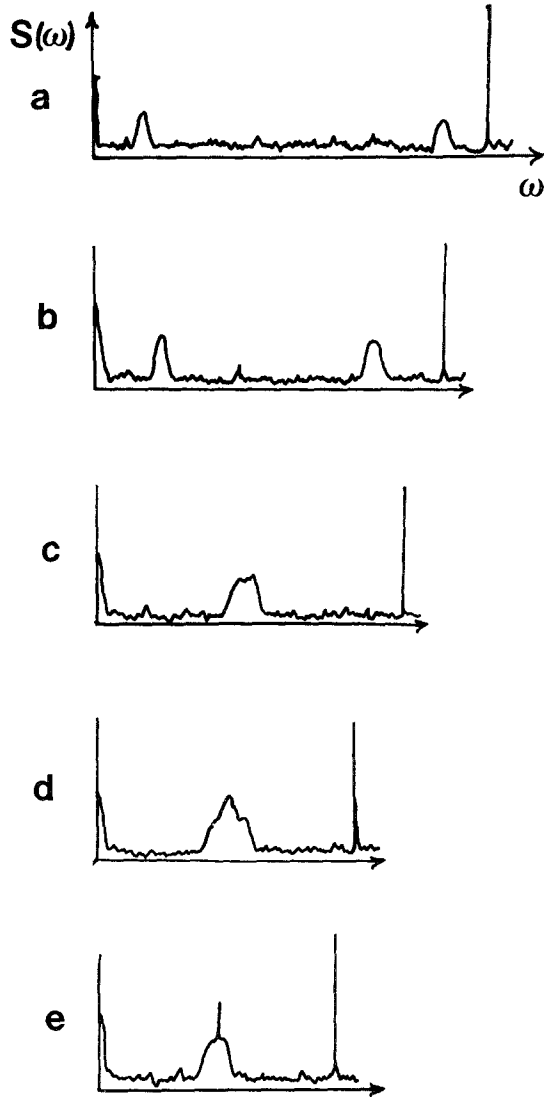

Fig. 1. Qualitative sketch of a typical sequence of power spectra for the nonlinear circuit studied in Ref. 1, as an external parameter is varied. The onset of period doubling occurs somewhere between Fig. 1c and Fig. 1e.

results from an experiment performed on a driven p–n junction.[12] In contrast, this paper does not deal with asymptotic scaling laws in the approach to chaos—the focus on the simplest instabilities broadens the relevance of this work to nonlinear systems that may or may not display chaotic behavior for some range of parameters.

Work more directly relevant to the present paper may be found in the laser literature. These studies considered the effects of noise on the power spectra near the onset of a *single* instability, although they confined themselves to the dynamical equations directly relevant to laser systems.[13–15] That body of work focused on the very first instability, the onset of lasing. The present work is broader in scope, and points out the general nature of the noisy power spectra for any sort of dynamical system. This comment is not meant to minimize the laser work: those theories[13,14] are based on a fully microscopic (quantum mechanical) physical description, and experimental evidence[15] shows that those analyses are substantially correct. In contrast, the present work begins with the (classical) ordinary differential equation (1), which is often (though not always) the starting point of a phenomenological description. On the other hand, the lesson taught by this paper is that, quite generally, the "noisy precursors" are a direct consequence of the existence of a (nearby) dynamical instability.

The body of the paper is organized as follows. In Section 2, we introduce a simple picture to motivate and define the mathematical model for external noise. The formal solution of this model is presented in Section 3, and the expected power spectrum for each class of codimension-one instability is derived on a case by case basis in Section 4: Figures 3–7 summarize these formal results. Two specific examples illustrating the main features of the analysis are presented in Section 5. Finally, a discussion of the limitations and conclusions of the present work is given in Section 6.

2. MODELING THE NOISE

The purpose of this section is twofold. First, we have to decide how to mathematically model the interaction of a system with external perturbations. Second, the simple picture we will use to guide our choice of model will enable us to anticipate, in an intuitive fashion, the main result of this paper. This heuristic reasoning will find its formal justification in Sections 3 and 4.

We begin by motivating the model. Consider a dynamical system described by the system of differential equations

$$\dot{\mathbf{x}} = \mathbf{F}(\mathbf{x}, t), \qquad \mathbf{x} \in \mathbb{R}^N \tag{1}$$

where $\mathbf{F}$ may or may not depend explicitly on time. (The system is said to

be nonautonomous or autonomous, respectively.) Suppose the system has an asymptotically stable T-periodic solution $\mathbf{x}_0$:

$$\mathbf{x}_0(t+T) = \mathbf{x}_0(t) \tag{2}$$

This solution describes a closed orbit in phase space, with nearby orbits approaching $\mathbf{x}_0$ as time increases. Imagine that a small perturbation kicks the system off of the limit cycle—it then relaxes back to the periodic orbit. For small perturbations, the transient $\boldsymbol{\eta} = \mathbf{x} - \mathbf{x}_0$ is governed by the dynamical equation (1) linearized about $\mathbf{x}_0$,

$$\dot{\boldsymbol{\eta}} = \mathbf{DF}(\mathbf{x}_0) \cdot \boldsymbol{\eta} \tag{3}$$

where $\mathbf{DF}$ is the matrix of periodic functions

$$(\mathbf{DF})_{ij} = \left. \frac{\partial F_i}{\partial x_j} \right|_{\mathbf{x} = \mathbf{x}_0} \tag{4}$$

When an instability is approached as some parameter varies, the relaxation time increases, and the transient response contributes more to the observed output. It is the contribution of the transients that we want to focus on as the external noise continually kicks the system away from the limit cycle. In this picture, the noise enters as a stochastic forcing term, so that (3) becomes

$$\dot{\boldsymbol{\eta}} = \mathbf{DF}(\mathbf{x}_0) \cdot \boldsymbol{\eta} + \boldsymbol{\xi}(t) \tag{5}$$

where ξ is taken for convenience to be Gaussian white noise:

$$\langle \boldsymbol{\xi}(t) \rangle = 0, \qquad \langle \xi_i(t)\, \xi_j(t+\tau) \rangle = \kappa_{ij}\, \delta(\tau) \tag{6}$$

Equation (5) is our starting point for analyzing the effect of noise on periodic nonlinear systems. As discussed in Section 6, there is a limit as to how well a linearized equation (5) can capture the nonlinear dynamics of the system. Furthermore, this is not the only way the noise might be modeled. Another way is to let the parameters of the system (1) fluctuate, in which case the phase space portraits fluctuate. The present model is a more static picture—the phase space portraits are frozen in, and the point representing the instantaneous state of the system is subject to external kicks. The situation is akin to a ball rattling around on a roulette wheel.

What can we expect to come out of an analysis based on this model? For definiteness, consider the case where the stable orbit $\mathbf{x}_0$ is close to undergoing a period-doubling bifurcation. The situation is depicted in Fig. 2, in which a Poincaré section is taken transverse to the periodic orbit.

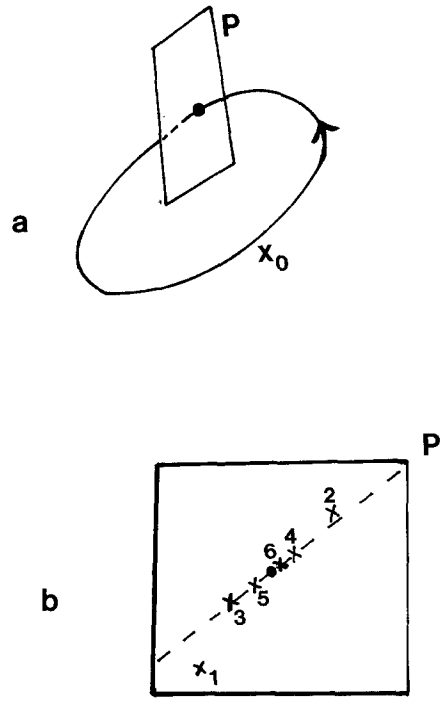

Fig. 2. (a) A Poincaré section P is taken transverse to the closed phase space orbit corresponding to the periodic solution $\mathbf{x}_0$. (b) Successive intersections of a trajectory relaxing back to the stable limit cycle $\mathbf{x}_0$.

This orbit is represented by a fixed point of the return map P. Figure 2b shows successive iterates of an orbit relaxing back to the stable limit cycle—close to a period-doubling instability, the iterates approach the fixed point in an alternating fashion. (It is for precisely this reason that a period-doubling instability is sometimes called a "flip bifurcation" in the bifurcation theory of discrete mappings.)[16] The transients therefore have the character of a damped, $2T$-periodic orbit, and the power spectrum should show a broad bump peaked at half the fundamental frequency of $\mathbf{x}_0$. This is the origin of the precursor exhibited in Fig. 1d.

Equation (5) is linear with periodic coefficients, and may be solved with the help of results from Floquet theory.[17] In fact, we construct a complete solution to this model in the next section. In the vicinity of a bifurcation, a great simplification is possible, and leads us to a classification scheme for the observed noisy power spectra corresponding to each type of instability, of which the period-doubling bifurcation is but one example.

3. FORMAL SOLUTION

We now construct the solution of Eq. (5). We consider real equations only, so the perturbation $\boldsymbol{\eta}(t)$ and the autocorrelation functions $C_{nm}(\tau)$ are real. However, in applying the results of Floquet theory, the introduction of complex functions offers such a great computational advantage that the derivations in this paper will be performed using complex notation. From Floquet theory, we know several facts.

First, there is a set of linearly independent solutions $\boldsymbol{\phi}^k$ of the *homogeneous* equation associated with Eq. (5), of the form

$$\boldsymbol{\phi}^k(t) = e^{\rho_k t}\boldsymbol{\chi}^k(t) \tag{7}$$

where the $\boldsymbol{\chi}^k$ are periodic functions with the same period as $\mathbf{DF}(\mathbf{x}_0)$. For convenience, we assume that time is scaled so that this period is 2π. Because the Floquet exponents ρ_k play a central role in the derivation and subsequent interpretation of the results, it is worthwhile to pause and discuss their basic properties. The ρ_k are, in general, complex numbers, and stability of the orbit $\mathbf{x}_0$ requires that $\operatorname{Re}\rho_k < 0$ for all k. The imaginary part of ρ_k is to some extent arbitrary—from Eq. (7) we see that ρ_k is determined only up to an integer multiple of i. (Rather than thinking of the ρ_k as lying in the complex plane, one should think of them as lying on a *cylinder*, with the imaginary axis wrapped around the "waist" of the cylinder.) We will eliminate this ambiguity in $\operatorname{Im}\rho_k$ by fixing

$$-\tfrac{1}{2} < \operatorname{Im}\rho_k \leqslant \tfrac{1}{2} \tag{8}$$

We are considering *real* differential equations (1), so the ρ_k naturally fall on the line $\operatorname{Im}\rho = 0$, or the line $\operatorname{Im}\rho = 1/2$, or they occur in complex conjugate pairs. Finally, as the parameters of the system are varied, the ρ_k move around on the complex cylinder—an instability occurs when one or more of the ρ_k cross the imaginary axis.

Returning to the main line of development, we will assume that all N Floquet exponents are distinct. In this case, we are guaranteed a complete set of N linearly independent solutions $\boldsymbol{\phi}^k$.

The $\boldsymbol{\phi}^k$ may be used to form a fundamental matrix $\boldsymbol{\Phi}(t)$ for the system (5):

$$\boldsymbol{\Phi}(t) = [\boldsymbol{\phi}^1(t), \boldsymbol{\phi}^2(t), \ldots, \boldsymbol{\phi}^N(t)] \tag{9}$$

so that $\boldsymbol{\phi}^k$ forms the kth column of $\boldsymbol{\Phi}(t)$. If $\boldsymbol{\Phi}(0)$ is nonsingular, then we are guaranteed that $\boldsymbol{\Phi}(t)$ remains nonsingular: we can always choose $\boldsymbol{\Phi}(0)$ to be invertible, hence its inverse $\boldsymbol{\Phi}^{-1}$ exists for all t.

The importance of the fundamental matrix is that the general solution of Eq. (5) may be expressed as

$$\boldsymbol{\eta}(t) = \boldsymbol{\Phi}(t) \int_0^t \boldsymbol{\Phi}^{-1}(t')\, \xi(t')\, dt' \tag{10}$$

In writing Eq. (10), we have assumed the homogeneous initial conditions $\boldsymbol{\eta}(0) = 0$. This is an unimportant restriction—our results are insensitive to the particular choice of initial conditions.

From Eq. (10), we arrive at once at the expected result that $\langle \boldsymbol{\eta}(t) \rangle = 0$. We now proceed to the (general) second moment $\langle \boldsymbol{\eta}_m(t)\, \boldsymbol{\eta}_n(t+\tau) \rangle$. First, rewrite Eq. (10) in component form

$$\eta_m(t) = \sum_r \Phi_{mr}(t) \sum_s \int_0^t \Phi_{rs}^{-1}(t')\, \xi_s(t')\, dt' \tag{11}$$

Using Eq. (6), the second moment reduces to

$$\langle \eta_m(t)\, \eta_n(t+\tau) \rangle = \sum_{rk} \Phi_{mr}(t)\, \Phi_{nk}(t+\tau) \int_0^t \sum_{sl} \kappa_{sl} \Phi_{rs}^{-1}(t')\, \Phi_{kl}^{-1}(t')\, dt' \tag{12}$$

To make further progress, it is necessary to examine more closely the fundamental matrix $\boldsymbol{\Phi}(t)$ and its inverse $\boldsymbol{\Phi}^{-1}(t)$. From Eqs. (7) and (9), we can express $\boldsymbol{\Phi}$ as the set of column vectors

$$\boldsymbol{\Phi}(t) = [e^{\rho_1 t} \boldsymbol{\chi}^1(t), \ldots, e^{\rho_N t} \boldsymbol{\chi}^N(t)]$$

so that

$$\Phi_{mr} = e^{\rho_r t} \chi_{mr} \tag{13}$$

where χ_{mr} is the mth component of $\boldsymbol{\chi}^r$. It follows that the inverse matrix may be written as the set of *row* vectors

$$\boldsymbol{\Phi}^{-1}(t) = \begin{pmatrix} e^{-\rho_1 t} \boldsymbol{\psi}_1(t) \\ \vdots \\ e^{-\rho_N t} \boldsymbol{\psi}_N(t) \end{pmatrix}$$

so that

$$\Phi_{rs}^{-1} = e^{-\rho_r t} \psi_{rs} \tag{14}$$

where

$$\boldsymbol{\chi}^k(t) \cdot \boldsymbol{\psi}_l(t) = \delta_{kl} \tag{15}$$

Equation (15) ensures that the matrix (14) gives the inverse of matrix (13). The vector functions χ and ψ are (possibly complex) 2π-periodic functions. Next, express the exponents ρ_k as the sum of real and imaginary parts:

$$\rho_k = a_k + ib_k \tag{16}$$

Using Eqs. (13), (14), and (16), the ensemble average Eq. (12) may be written

$$\langle \eta_m(t)\, \eta_n(t+\tau) \rangle = \sum_{rk} h_{mr}(t)\, h_{nk}(t+\tau)\, e^{a_k \tau} \int_0^t e^{(a_k + a_r)(t-t')} \left[\sum_{sl} \kappa_{sl}\, g_{rs}(t')\, g_{kl}(t') \right] dt' \tag{17}$$

where

$$h_{mr}(t) \equiv e^{ib_r t} \chi_{mr}(t) \tag{18}$$

and

$$g_{rs}(t') \equiv e^{-ib_r t'} \psi_{rs}(t') \tag{19}$$

are *bounded*, though not necessarily periodic, functions of time.

It should be emphasized that Eq. (17) is an exact consequence of Eq. (5).

Equation (17) is the main result of this section, and is the starting point for examining various special cases in Section 4.

We now make the important observation that, *near an instability, an enormous simplification of Eq.* (17) *is possible.* So far, we have been able to discuss both autonomous and nonautonomous systems of the form Eq. (1) simultaneously—we must now draw an important distinction between the two cases.

First consider the nonautonomous case. Then near an instability, a single Floquet exponent ρ_1—or a complex conjugate pair ρ_1, ρ_2—has a small (negative) real part, while all other exponents ρ_k have relatively large (negative) real part

$$a_1/a_k \ll 1 \tag{20}$$

Since the integrand in Eq. (17) is the product of a decaying exponential and a bounded, oscillating function, the $r = 1$, $k = 1$ term dominates the expression for large t. It is the properties of this dominant term which lead to the main noisy precursor results for the power spectrum.

Now consider the autonomous case—here the system is constrained to always have a zero exponent, say, $\rho_N = 0$. Geometrically, this corresponds

to the fact that the flow in phase space is neutrally stable to perturbations along the periodic orbit. Near an instability, we again have a_1 small, but now we retain four terms in Eq. (17): $(r, k) = (N, N)$, $(N, 1)$, $(1, N)$, and $(1, 1)$. The first three of these add features that are not present in the nonautonomous case; they essentially serve to broaden the δ-function power spectrum from the basic periodic orbit $\mathbf{x}_0$. Rather than pause here to compute their effect, we postpone the details until the Appendix.

Keeping in mind this basic distinction between the autonomous and nonautonomous problems, we are now ready to unveil the noisy power spectrum characteristic of each of the codimension-one bifurcations.

4. PRECURSORS OF CODIMENSION-ONE INSTABILITIES

According to bifurcation theory,[16] the periodic orbit $\mathbf{x}_0$ generically loses stability in one of three ways as a single parameter is varied—such instabilities are called codimension-one bifurcations:

(i) A single ρ_k crosses into the right half-cylinder along the real axis. In a deterministic analysis, one usually distinguishes three subcases according to the symmetry and so-called nondegeneracy conditions of the problem. For our purposes, only the symmetry considerations play a special role—we will therefore consider separately the unsymmetric case (corresponding to the saddle-node and transcritical bifurcations) and the symmetric case (corresponding to the pitchfork bifurcation).

(ii) A single ρ_k crosses into the right half-cylinder along the line $b = 1/2$. This corresponds to a period-doubling instability.

(iii) A pair of complex conjugate ρ_k cross into the right half-cylinder. This is often called a Hopf bifurcation, and corresponds to the onset of "motion on an invariant two-torus" (provided certain "strong resonances" are avoided[16])—that is, either phase locked or quasiperiodic oscillations.

In each of these cases, we consider the expected power spectrum *before* the instability occurs, so that the basic orbit $\mathbf{x}_0$ is still stable. The results give us the characteristic "noisy precursor" spectrum corresponding to each class of codimension-one bifurcation.

4.1. Saddle-Node or Transcritical Precursor

We suppose that

$$\varepsilon \equiv |a_1| \ll 1, \qquad b_1 = 0 \tag{21}$$

and all the other ρ_k have relatively large negative real part [see Eq. (20)]. The instability is signaled when $\rho_k = 0$. Retaining only the dominant $r = 1$, $k = 1$ term, Eq. (17) reduces to

$$\langle \eta_m(t)\, \eta_n(t+\tau) \rangle = h_{m1}(t)\, h_{n1}(t+\tau)\, e^{-\varepsilon\tau} \int_0^t e^{-2\varepsilon(t-t')} \left[\sum_{sl} \kappa_{sl}\, g_{1s}(t')\, g_{1l}(t') \right] dt' \quad (22)$$

In any measurement of a power spectrum, one needs to take a time series of much longer duration than any relevant characteristic time of the system being studied. We therefore consider the ordering

$$t \gg \varepsilon t \gg 2\pi \quad (23)$$

In this limit, we can find a simple expression for the integral appearing in Eq. (22). Since the $g_{1s}(t')$ are bounded 2π-periodic functions, we can express the term in square brackets as a Fourier sum:

$$\sum_{sl} \kappa_{sl}\, g_{1s}(t')\, g_{1l}(t') = \sum_{\nu=-\infty}^{\infty} Q_\nu e^{i\nu t'} \quad (24)$$

and the integral in Eq. (22) becomes approximately $Q_0/(2\varepsilon)$. This result is easy to understand: the integrand in Eq. (22) is the product of a bounded oscillation times a very slowly decaying exponential. For large t, we can extend the upper limit of integration to infinity. Then the integral is just the mean value Q_0 of the oscillation times the area $(2\varepsilon)^{-1}$ under the exponential. We thus have

$$\langle \eta_m(t)\, \eta_n(t+\tau) \rangle = \frac{Q_0}{2\varepsilon} h_{m1}(t)\, h_{n1}(t+\tau)\, e^{-\varepsilon\tau} \quad (25)$$

which depends on both t and τ. Consequently, the process described by Eq. (5) is nonstationary. This is not surprising, since the phase of the limit cycle $\mathbf{x}_0(t)$ distinguishes between different times t. In an operational sense, however, a spectrum analyzer performs both an ensemble average *and* a time average. (Typically, one takes a single time series and derives a power spectrum by performing time averages, and then repeats this operation on a sequence of different time series, adding the resulting power spectra.) Consequently, we may take the correlation function to be

$$C_{mn}(\tau) \equiv \overline{\langle \eta_m(t)\, \eta_n(t+\tau) \rangle}^t = \frac{Q_0}{2\varepsilon} \overline{h_{m1}(t)\, h_{n1}(t+\tau)}^t\, e^{-\varepsilon\tau} \quad (26)$$

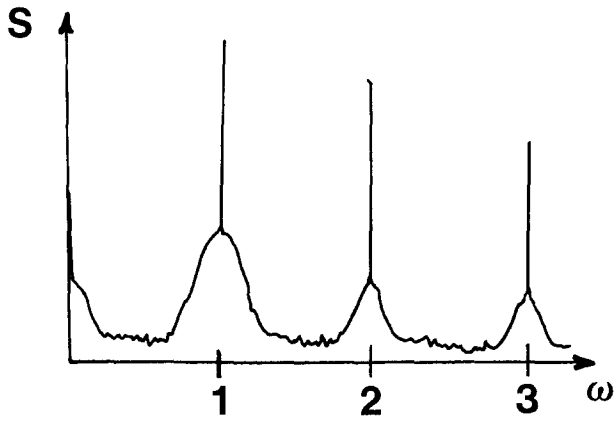

Fig. 3. Expected power spectrum in the vicinity of a saddle-node or transcritical instability.

The Fourier transform of $C_{mn}(\tau)$ gives the power spectrum $S_{mn}(\omega)$—expanding the 2π-periodic function in the Fourier series

$$\overline{h_{m1}(t)\, h_{n1}(t+\tau)}^{t} = \sum_{l=-\infty}^{\infty} \alpha_l e^{il\tau}, \qquad \alpha_{-l} = \alpha_l^* \tag{27}$$

we find

$$S_{mn}(\omega) = Q_0 \sum_{l=-\infty}^{\infty} \alpha_l [\varepsilon^2 + (\omega - l)^2]^{-1} \tag{28}$$

This sum of Lorentzians should be added to the δ-function spikes from the basic oscillation $\mathbf{x}_0(t)$ (and to the line-broadening features of these spikes present for autonomous systems). The resulting power spectrum is illustrated in Fig. 3.

4.2. Symmetry Breaking (Pitchfork) Precursor

This case is relevant when the governing equation (1) has the symmetry

$$\mathbf{F}(\mathbf{x}, t) = \mathbf{F}(-\mathbf{x}, t + T/2) \tag{29}$$

and the periodic solution shares this symmetry, namely,

$$-\mathbf{x}_0(t + T/2) = \mathbf{x}_0(t) \tag{30}$$

This symmetry is fairly common, and occurs for example in the case of a driven, damped pendulum

$$\mathbf{x} = \begin{pmatrix} \theta \\ \dot{\theta} \end{pmatrix}, \qquad \mathbf{F}(\mathbf{x}, t) = \begin{pmatrix} \dot{\theta} \\ -\gamma\dot{\theta} - \sin\theta + A\cos\omega t \end{pmatrix} \tag{31}$$

For small values of driving amplitude A, the solution to Eq. (1) is symmetric. It follows that the power spectrum of $\theta(t)$ contains only odd harmonics of the fundamental frequency—this is the experimental signature of a symmetric orbit. As A is increased, this system is known to undergo a cascade of period doublings leading to chaos.[18] Before the first period doubling, however, the system undergoes a symmetry-breaking bifurcation: the observed power spectrum develops some even harmonic content as the bifurcation point is passed.[19]

In general, we can expect to observe symmetry breaking in symmetric systems before period doubling.[19–22] We now examine the effect of noise on the power spectrum near a symmetry-breaking bifurcation.

In fact, the details of this case are identical to those of Section 4.1, all the way up to the final result for the noisy power spectrum Eq. (28). The only difference is that the peaks of the Lorentzians do not coincide with the δ-function spikes contributed by the basic oscillation $\mathbf{x}_0$. To see this, recall that the derivation of the main result Eq. (17) assumed that the matrix $\mathbf{DF}(\mathbf{x}_0, t)$ [see Eq. (4)] had period 2π. Typically, we expect $\mathbf{DF}(\mathbf{x}_0, t)$ to have the same period as $\mathbf{x}_0$, but in the present symmetric case $\mathbf{x}_0$ has twice the period of $\mathbf{DF}$. For example, the pendulum Eqs. (1), (31) may be linearized about $\mathbf{x}_0(t)$ to give

$$\frac{d}{dt}\begin{pmatrix} \eta \\ \dot{\eta} \end{pmatrix} = \begin{pmatrix} 0 & 1 \\ -\cos\theta_0(t) & -\gamma \end{pmatrix}\begin{pmatrix} \eta \\ \dot{\eta} \end{pmatrix} \tag{32}$$

and since θ_0 simply changes sign after a half-period, the matrix has half the period of θ_0.

Since the result (28) was derived for $\mathbf{DF}$ being 2π-periodic, it follows that $\mathbf{x}_0(t)$ is 4π-periodic. The symmetry of $\mathbf{x}_0$ further implies that the basic oscillation contributes δ-function spikes at frequencies $\omega = 1/2,\ 3/2,\ 5/2, \ldots$.

Consequently, the noise-induced Lorentzians occur only in between these spikes. The situation is depicted in Fig. 4. Note that the noisy precursors appear precisely where the new even harmonic spikes are anticipated after the symmetry-breaking bifurcation has occurred.

4.3. Period-Doubling Precursor

In this case a single exponent approaches the imaginary axis with

$$a_1 = -\varepsilon, \qquad b_1 = \tfrac{1}{2}i \tag{33}$$

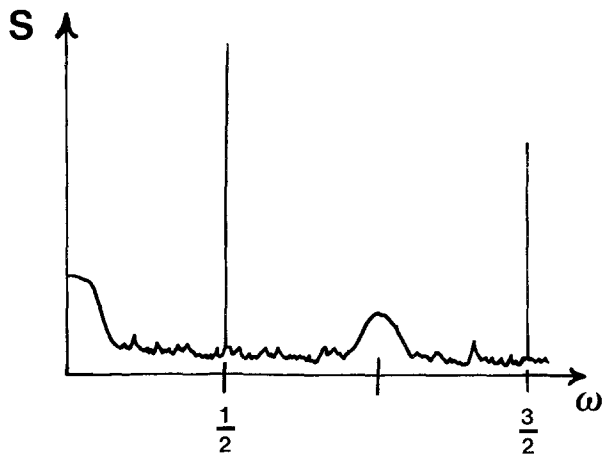

Fig. 4. Expected power spectrum in the vicinity of a symmetry-breaking (i.e., pitchfork) instability. The symmetry of the unperturbed orbit is reflected by the absence of spikes at even harmonic frequencies.

In Eq. (17), we retain only the $r=1$, $k=1$ term, and again arrive at Eq. (22). This time, however, the functions $h_{m1}(t)$ and $g_{m1}(t)$ have an additional property: they merely change sign after half a period, as can be seen from Eqs. (18) and (19). That is, they are symmetric functions in the sense of Eq. (30).

As before, the integral may be replaced by $Q_0/(2\varepsilon)$, and we are led once again to the resulting power spectrum (28), with a slight difference:

$$S_{mn}(\omega) = Q_0 \sum_{l\,\text{odd}} \alpha_l [\varepsilon^2 + (\omega - l)^2]^{-1} \tag{34}$$

The summation is restricted to odd l because the functions $h_{m1}(t)$ are symmetric near the period doubling, and thus the Fourier expansion (27) contains only odd-l terms.

The resulting power spectrum near the period-doubling instability is illustrated in Fig. 5. It is perhaps surprising that precursor bumps are not predicted at the integer frequencies $\omega = 0, 1, 2, \ldots$. The situation is very much like the symmetry-breaking precursor, even though the underlying equations need not have any symmetry for the period-doubling case.

(Because of the similarity between the period-doubling and symmetry-breaking precursor pictures, it is perhaps worth mentioning that symmetry breaking of discrete mappings may be thought of as period doubling of a related mapping—see Ref. 22 and 23 for details.)

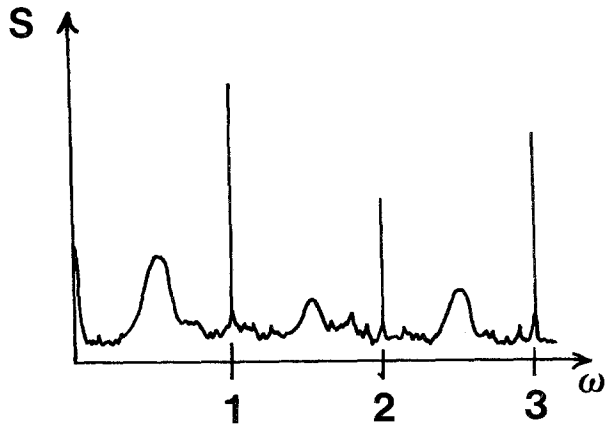

Fig. 5. Expected power spectrum in the vicinity of a period-doubling instability.

4.4. "Hopf" Precursor

This is the last case we shall consider. Here, a pair of complex conjugate ρ_k are near the imaginary axis:

$$\begin{aligned} \rho_1 &= -\varepsilon + ib \\ \rho_2 &= -\varepsilon - ib, \qquad 0 < b < \tfrac{1}{2} \end{aligned} \tag{35}$$

and their associated periodic functions χ^k are likewise complex conjugate, so that [see Eqs. (7) and (18)]

$$h_{m2}(t) = h_{m1}^*(t) \tag{36}$$

We now retain the four terms $(r, k) = (1, 1), (1, 2), (2, 1), (2, 2)$, in Eq. (17):

$$\langle \eta_m(t)\, \eta_n(t+\tau) \rangle = \sum_{r,k=1}^{2} h_{mr}(t)\, h_{nk}(t+\tau)\, e^{-\varepsilon\tau} \int_0^t e^{-2\varepsilon(t-t')} Q_{rk}(t')\, dt' \tag{37}$$

where

$$Q_{rk}(t') \equiv \sum_{sl} \kappa_{sl}\, g_{rs}(t')\, g_{kl}(t') \tag{38}$$

Again we can say that the integrals contribute some average factor:

$$\int_0^t e^{-2\varepsilon(t-t')} Q_{rk}(t')\, dt' \simeq \frac{\hat{Q}_{rk}}{2\varepsilon} \tag{39}$$

for the ordering given by Eq. (23).

Next, we perform an average over t. Now,

$$h_{m1}(t)\,h_{n1}(t+\tau) = e^{ibt}\chi_{m1}(t)\,e^{ib(t+\tau)}\chi_{n1}(t+\tau)$$
$$= e^{2ibt}[\chi_{m1}(t)\,\chi_{n1}(t+\tau)]\,e^{ib\tau} \tag{40}$$

and since $0 < b < 1/2$, and average over t gives zero. A similar argument shows that the last term in Eq. (37) vanishes upon taking the time average. Finally, we turn to the "cross-terms." Using Eq. (36),

$$h_{m1}(t)\,h_{n2}(t+\tau) + h_{m2}(t)\,h_{n1}(t+\tau) = 2\mathrm{Re}[e^{-ib\tau}\chi_{m1}(t)\,\chi^*_{n1}(t+\tau)] \tag{41}$$

Taking an average over t yields a periodic or quasiperiodic function of τ, with fundamental frequencies b and 1. The correlation function is

$$C_{mn}(\tau) = \frac{\hat{Q}_{12}}{\varepsilon}\,e^{-\varepsilon\tau}\,\mathrm{Re}[e^{-ib\tau}\overline{\chi_{m1}(t)\,\chi^*_{n1}(t+\tau)^t}] \tag{42}$$

This should be compared with Eq. (26)—the only difference is that the oscillating piece of Eq. (42) is a function of two (possibly incommensurate) frequencies. The power spectrum is again the convolution of a Lorentzian of width 2ε and a sequence of δ functions—this time the δ functions occur at the frequencies $l \pm b$, $l = 0, 1, 2, \ldots$. The resulting power spectrum is illustrated in Fig. 6.

The results of this section are summarized in Figs. 3–6. For each general class of instability, there is a characteristic noisy precursor. In

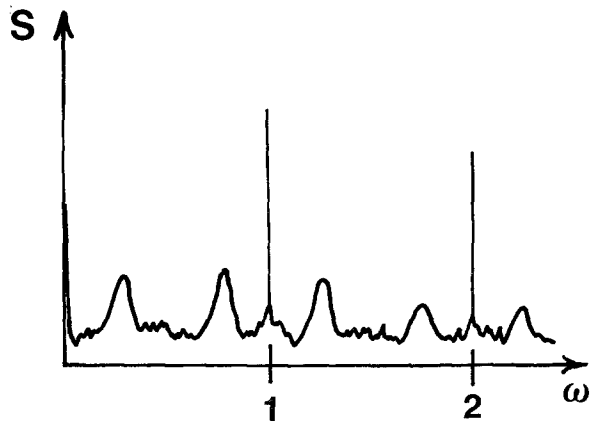

Fig. 6. Expected power spectrum in the vicinity of a Hopf instability. Here, the quantity b [see Eq. (16)] is about 1/3.

essence, we have simply followed the classification scheme for codimension-one bifurcations familiar from bifurcation theory of mappings, and have extended those results to include the effects of external noise.

5. EXAMPLES

In this section, the general features of the previous analysis are illustrated by two examples. Both examples have been the subject of previous experimental investigations. Before turning to these, however, it is useful to summarize the results of Section 4 in the following compact way.

The stability to a nonlinear dynamical system displaying periodic behavior is characterized by the (nonzero) Floquet exponents ρ_k: an instability occurs when one exponent, say, ρ_1 (or in the Hopf case, the pair ρ_1 and $\rho_2 = \rho_1^*$) crosses the imaginary axis. In the presence of noise, it is ρ_1 that characterizes the broad peaks appearing in the power spectrum. The *size and shape* of these peaks are governed by the real part of ρ_1 (see Fig. 7a), while the *position* of these peaks are governed by the imaginary part of ρ_1 (Fig. 7b). From Fig. 7b, we see that the precursor of the period-doubling instability ($b = 1/2$) can be thought of as a special case of the general Hopf precursors ($0 < b < 1/2$).

5.1. Example One: The Driven Pendulum and the Swift Criterion

This system, described by Eq. (31), has been studied in detail on analog electrical circuits.[18,19] As mentioned in the last section, as the drive amplitude A is increased from zero, the system undergoes a symmetry-breaking bifurcation, followed by a sequence of period-doubling instabilities leading to chaos. As the system is driven even harder, other instabilities occur, but here we want to focus on the expected power spectra, in the presence of noise, up through the first period doubling.[24]

Figures 8a–e show a sequence of power spectra for increasing A, for a drive frequency $\omega = 1$. Observe that the noisy precursor bumps occur right where the not-yet-born bifurcated solution has new spikes. This demonstrates a basic difficulty encountered when trying to precisely determine the critical parameter value for the onset of dynamical instability.

It should be pointed out that the "precursor" bumps *do not* disappear immediately after the bifurcation occurs, but gradually subside. Thus, since the $\omega = 1/2$ spike grows continuously from zero height for a period-doubling instability, one must sweep some finite amount past criticality to pick out the spike above the noisy background peak. A practical criterion for experimentally determining the critical parameter value has been suggested

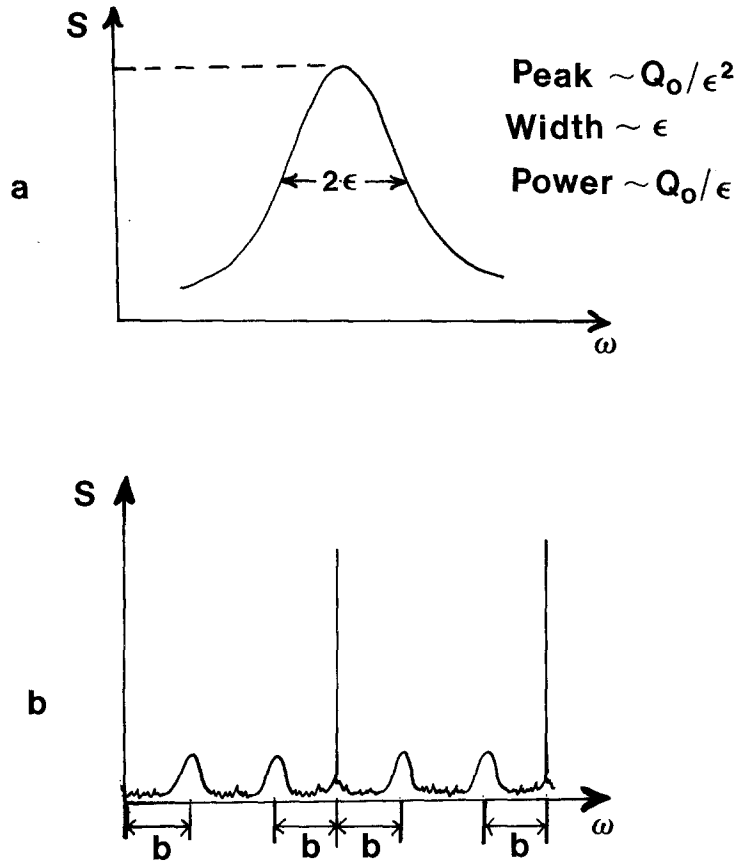

Fig. 7. (a) Scaling for the Lorentzian precursor peaks. The Floquet exponent $\rho_1 = -\varepsilon + ib$, $-1/2 < b \leqslant 1/2$. (b) The position of the precursor peaks is a function of b. The large spikes are due to the basic oscillation $\mathbf{x}_0$.

by James Swift.[25] The idea is to first sweep past the instability until the spike is clearly visible above the background. Since the amplitude of the period-doubled solution grows as the square root of the bifurcation parameter close enough to the instability,[16] the power grows linearly, so one can then decrease the parameter and extrapolate to find the point where the new peak has zero amplitude.

Note that the Swift criterion does not depend on the detailed scaling of the noise peaks derived here (which, as discussed in Section 4, must break down close enough to the instability), since it relies only on the deterministic elements of the bifurcation analysis.

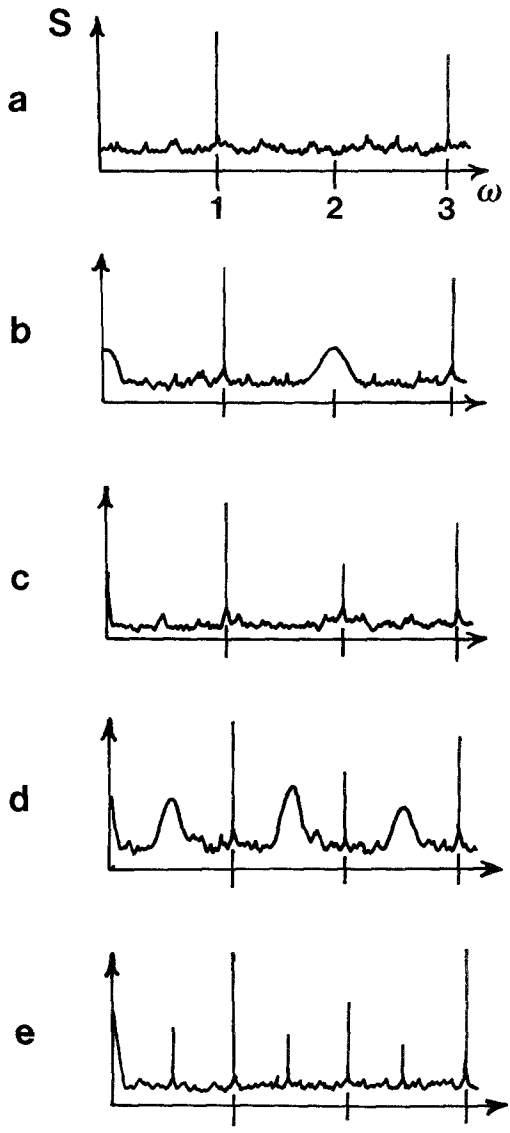

Fig. 8. Expected sequence of power spectra for the driven pendulum as a function of increasing drive amplitude, up through the first period doubling. The solution must undergo symmetry breaking (Fig. 8c) before period doubling (Fig. 8e).

5.2. Example Two: A Josephson Junction Circuit

We have stressed that the Floquet exponents ρ_k play the central role in determining the observed power spectrum. Unfortunately, it is usually very difficult to actually compute the ρ_k from the governing dynamical equation. The main reason for this is that one must first find a periodic solution $\mathbf{x}_0$ to the nonlinear differential equation—a notoriously difficult task. Since one linearizes the basic equation about this solution, small errors in the expression for $\mathbf{x}_0$ can get magnified substantially in the ensuing stability analysis.

Happily, there is a system that displays a period-doubling instability which can be accurately analyzed with a modicum of effort. This system is a nonlinear circuit involving a Josephson junction with a resistive shunt. If the self-inductance of the shunt is ignored and the circuit is driven with an ac bias current, the system is well described by the driven pendulum equation (31).[26,27] However, if the shunt has nonnegligible self-inductance, and the system is driven by a dc bias current, the appropriate evolution equation is (in dimensionless form):

$$\beta_L \beta_C \dddot{\delta} + \beta_C \ddot{\delta} + \dot{\delta}(1 + \beta_L \cos\delta) + \sin\delta = I \tag{43}$$

where $\dot{\delta}$ is proportional to the voltage across the junction, and β_L, β_C, and I are three dimensionless parameters measuring the inductance, capacitance, and bias current, respectively. The original experiments on real junctions showed the existence of a variety of time-dependent modes depending on the parameter values.[28,29] Subsequent simulations using an analog circuit demonstrated that Eq. (43) accurately modeled the junction over a wide range of parameter values.[30] More recently,[1] analytic headway was reported concerning a period-doubling instability observed in the system—comparisons with digital integration of Eq. (43) and with measurements made on the analog circuit showed that even fairly crude analytic approximations predicted $\mathbf{x}_0$ and the onset of period doubling to within a few per cent. The reason for this success is that, as I is lowered from a high value, the oscillations in $\dot{\delta}(t)$ have very little harmonic content. Therefore, only one or two terms in a Fourier expansion for $\dot{\delta}$ is sufficient to give good accuracy.

Because of the demonstrated accuracy of the analytic work, this system is ideal for computing the exponents ρ_k as a function of the parameter values β_L, β_C, and I. Here is a brief outline of the method used to compute the ρ_k. Begin by putting

$$\delta_0 = jt + A\sin(jt + \phi) \tag{44}$$

into the evolution equation (43). The unknown quantities j, A, and ϕ are determined by separately balancing coefficients of the constant, $\sin jt$, and $\cos jt$ terms, while ignoring all higher harmonics. This determines the basic periodic solution of Eq. (43).

Next, linearize Eq. (43) about δ_0:

$$\beta_L\beta_C\dddot{\eta}+\beta_C\ddot{\eta}+\dot{\eta}[1+\beta_L\cos\delta_0(t)]+\cos\delta_0-\beta_L\dot{\delta}_0\sin\delta_0=0 \quad (45)$$

where $\eta=\delta-\delta_0$. We rescale time so that the linearized equation has coefficients of period 2π: let $\tau=jt$, then

$$j^3\beta_L\beta_C\eta'''+j^2\beta_C\eta''+j[1+\beta_L\cos\delta_0(\tau)]+\cos\delta_0(\tau)-j\beta_L\delta_0'\sin\delta_0=0 \quad (46)$$

where the primes denote differentiation with respect to τ. This has solutions of the form

$$\eta_k=e^{i\rho_k\tau}P_k(\tau) \quad (47)$$

where $P_k(\tau+2\pi)=P_k(\tau)$. This suggests Fourier expanding $P_k(\tau)$ and substituting the resulting η_k into Eq. (46). Since Eq. (46) is linear, this substitution yields (by balancing coefficients of each harmonic) a set of linear algebraic equations, which may be written in the matrix form

$$\mathbf{M}\cdot\boldsymbol{\alpha}=0 \quad (48)$$

where the α_m are the coefficients of the Fourier expansion for $P_k(\tau)$, and the coefficient matrix $\mathbf{M}$ depends on ρ_k. The ρ_k are determined by the condition

$$\text{DET } M(\rho_k)=0 \quad (49)$$

which may be solved numerically. The results displayed on the right-hand side of Fig. 9 were produced in an afternoon's work using an HP-15 calculator, for $\beta_L=3.0$, $\beta_C=0.1$, and five values of I. (Past experience has shown that the calculations work particularly well in this parameter range.) Once the exponents are computed, we can use the results of this paper to deduce the position and the width of the Lorentzian noise peaks. The expected power spectra are drawn on the left-hand side of Fig. 9—the relative heights of the precursor bumps have been chosen arbitrarily.

We can understand these results in the following way. Since this is an autonomous system, one Floquet exponent is fixed at zero:

$$\rho_3=0 \quad (50)$$

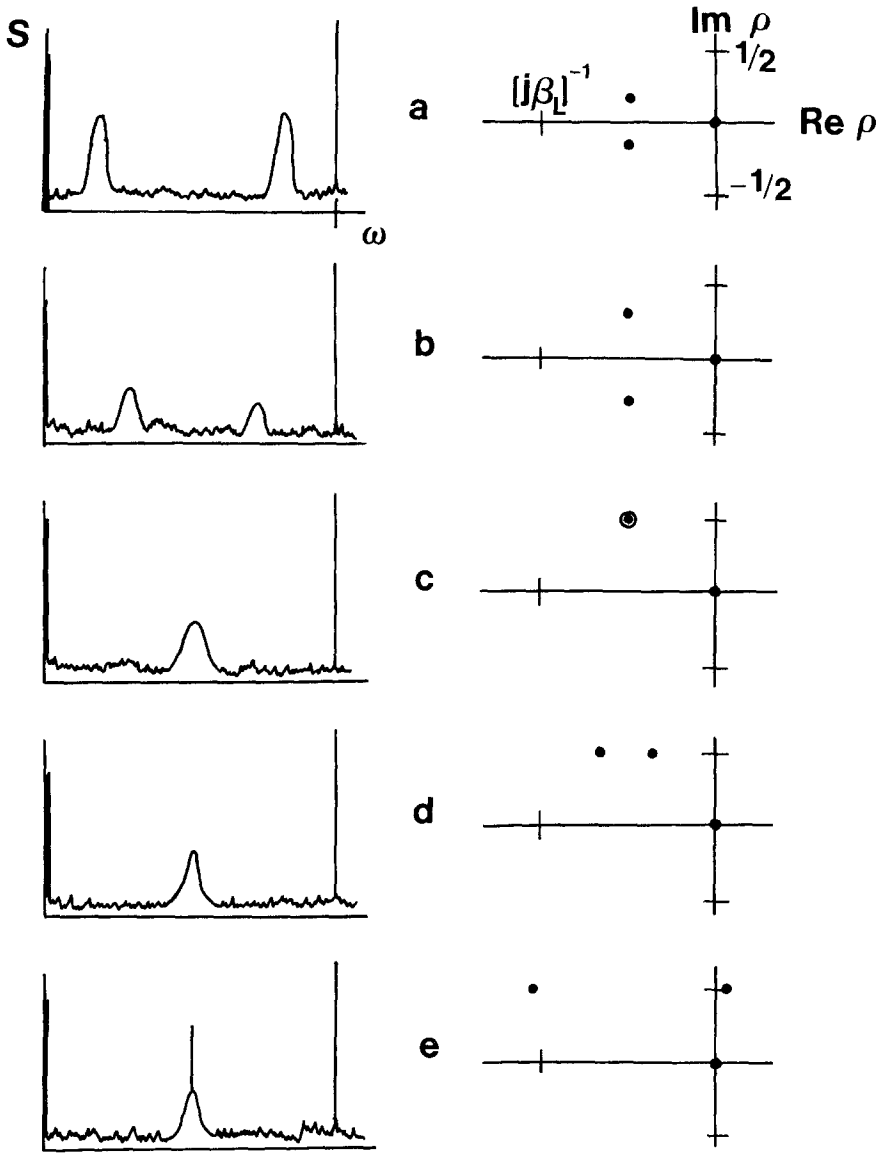

Fig. 9. Calculated values of the Floquet exponents (right-hand side) for the Josephson circuit governed by Eq. (43), and the corresponding expected power spectra (left-hand side). The exponents were computed for $\beta_L = 3.0$, $\beta_C = 0.1$, and $I = 10.0$, 7.5, 5.1, 5.0, and 4.9, for parts a–e, respectively. The "bulls-eye" symbol in Fig. 8c indicates that two Floquet exponents coincide at $\rho = [2j\beta_L]^{-1} + i/2$.

—the observed period-doubling instability occurs when one of the exponents is equal to $(1/2)i$. For any system, there is always one constraint on the sum of all N Floquet exponents[17]—in the present case, this constraint is [in view of Eq. (50)]

$$\rho_1 + \rho_2 = -(j\beta_L)^{-1} \tag{51}$$

Thus, either $\operatorname{Im}\rho_1 = \operatorname{Im}\rho_2 = 0$, or $\operatorname{Im}\rho_1 = \operatorname{Im}\rho_2 = 1/2$ [recall the discussion preceding Eq. (7)], or

$$\rho_1 = \rho_2^* = -\frac{1}{2j\beta_L} + ib, \qquad 0 < b < \frac{1}{2} \tag{52}$$

In the limit of large I, one can show that, in general, $\operatorname{Im}\rho_1 = (I^2\beta_L\beta_C)^{-1/2}$, which is about 0.183 for these parameter values (Fig. 9a). Physically, the nonlinear element is effectively out of the circuit at large bias currents I, and this corresponds to the resonant frequency of the remaining simple LC circuit. As I is decreased, the coupling with the nonlinear element shifts this frequency, thus the imaginary part of the exponents change (Fig. 9b) until ρ_1 and ρ_2 meet at $\rho = -(2j\beta_L)^{-1} + i/2$ (Fig. 9c—recall that the lines $\operatorname{Im}\rho = -1/2$ and $\operatorname{Im}\rho = +1/2$ are identified). Note that as the bumps in the power spectrum shift position, their relative widths increase. This follows from Eq. (52): j decreases as I decreases, and the real part of the Floquet exponents determines the width and height of the precursor lines (see Fig. 7a). Once the exponents meet, they split apart along the line $\operatorname{Im}\rho = 1/2$ (Fig. 9d), and period doubling occurs when $\rho_1 = i/2$ [and so $\rho_2 = -1/(j\beta_L) + i/2$]. Figure 9e is drawn a little bit past the onset of period doubling.

It is interesting to note that the power spectrum in Fig. 9b corresponds to the noisy precursor near a Hopf bifurcation (compare Fig. 6) even though no Hopf bifurcation occurs. In a sense, the system *is* near a Hopf bifurcation; however, the constraint (51) and the physical restriction that β_L remain finite prohibit the Hopf bifurcation from occurring.

6. LIMITATIONS AND CONCLUSIONS

In this paper we have examined the effect of external noise on the power spectrum of systems near an instability of a periodic orbit. We have looked at this problem within the context of a specific model for the noise, and found it possible to characterize the main features expected as a single parameter is varied. Our findings essentially extend the results familiar from the usual classification scheme of codimension-one bifurcations of discrete mappings.[16] We emphasize that the results depend only on the type of dynamical instability involved, independent of the physics behind the

governing differential equation (1). The wide occurrence of codimension-one bifurcations in nonlinear systems, and the ubiquity of noise, leads us to expect the observation of these noisy precursors in most experiments on dynamical instabilities of periodic orbits.

We now finish by pointing out the limitations of the theory presented above. The most serious is the linearization of the equation for the perturbation η. Consider a system with fixed noise strength: as the instability is approached, the relaxation time increases, and the perturbation can grow in magnitude to the point where nonlinear terms are important. As a result, the scaling summarized in Fig. 7a will necessarily break down close enough to the instability.

A second limitation concerns the basic assumption of Section 4, namely, that either a single or complex conjugate pair of "near critical" Floquet exponents dominate(s) the resulting power spectrum. This assumption, which is expressed quantitatively by the inequality (20), will be valid sufficiently close to the instability. In that sense, this approximation is complementary to the linearization approximation—for a particular problem, however, it may happen that there is no range of parameter values where both the linearization and inequality (20) are simultaneously valid. This potential difficulty seems particularly likely in systems with a very large number of Floquet exponents—that is, if the original equation (1) is a high-dimensional system. In that event, however, a different approach may prove fruitful. Going back to Eq. (17), which represents an exact solution of Eq. (5), we can approximate the sum as a weighted integral over the statistical distribution of Floquet exponents. However, it is an open question whether, given some large system of differential equations with a periodic solution, one can *a priori* say anything about the distribution of the ρ_k.

Lastly, we reiterate that the present approach is not the only way to model the effect of external fluctuations. One alternative would be to allow the *parameters* to fluctuate—rather than studying the additive noise problem defined by Eq. (5), the governing equation would involve multiplicative noise. For some problems we expect that this approach would model the physics better than the present theory. Experience shows, furthermore, that multiplicative noise can lead to dramatically different results than the additive noise counterpart.[31,32] The primary difficulty with the multiplicative noise model is that the governing equation does not have periodic coefficients, so that the machinary of Floquet theory so heavily relied upon here is of no use. On the other hand, recent work by L. Arnold[33] on the computation of Lyapunov exponents for linear stochastic differential equations seems to give the extension of concepts necessary to tackle the multiplicative noise case.

ACKNOWLEDGMENTS

The original insight as to the origin of the noisy precursors is due to James Swift. The author acknowledges useful discussions with W. Jagy, R. F. Miracky, J. W. Swift, and especially E. Knobloch. Also important was the encouragement of N. B. Abraham, J. Clarke, C. D. Jeffries, and W. C. Schieve.

APPENDIX

The purpose here is to examine the contribution to Eq. (17) due to a zero Floquet exponent. As mentioned in Section 3, the importance of this case lies in their fact that an autonomous system possessing a limit cycle *always* has a zero exponent ρ_N. The noisy precursors derived in Section 4 will have additional features for autonomous systems, owing to the terms $(r, k) = (N, N)$, $(1, N)$, and $(N, 1)$ appearing in Eq. (17). We examine each of these in turn.

$r = N, k = N$. The geometric interpretation of the zero Floquet exponent is that the limit cycle $\mathbf{x}_0$ is neutrally stable to perturbations along the orbit. In driven systems, the external forcing singles out a particular phase of the oscillation; conversely, for autonomous systems, perturbations cause the phase of the orbit to execute a random walk. This "phase diffusion" serves to broaden the δ-function spikes in the power spectrum due to $\mathbf{x}_0$. We remark that a straightforward evaluation of the $r = N$, $k = N$ term in Eq. (17) leads to unbounded growth proportional to t—this simply reflects the fact that the variance of the phase fluctuations grows with time, just as in any linear diffusion process. The divergence of this expression is of no concern, since it is obvious that our perturbative analysis is inappropriate for this effect—it is rightfully treated as a line broadening of the main δ-function spikes. We also observe that this effect is independent of ε, and so does not change as the deterministic parameters are varied.

$r = 1$, $k = N$. From Eq. (17), this term is

$$h_{m1}(t)\, h_{nN}(t+\tau) \int_0^t e^{-\varepsilon(t-t')} \left[\sum_{sl} \kappa_{sl}\, g_{1s}(t')\, g_{Nl}(t') \right] dt' \tag{A1}$$

For the ordering given by Eq. (23), the integral may be evaluated in terms of the mean value Q_0 of the oscillating factor in the integrand, and expression (A1) becomes

$$h_{m1}(t)\, h_{nN}(t+\tau) \frac{Q_0}{\varepsilon} \tag{A2}$$

The power spectrum corresponding to (A2) is a sequence of δ functions at $\omega = 0, 1, 2, \ldots$, which adds to the δ-function spikes already present owing to the basic oscillation $\mathbf{x}_0$. We note that this effect *does* depend on ε.

$r = N$, $k = 1$. This term is

$$h_{mN}(t)\, h_{n1}(t+\tau)\, e^{-\varepsilon\tau} \int_0^t e^{-\varepsilon(t-t')} \left[\sum_{sl} \kappa_{sl}\, g_{Ns}(t')\, g_{1l}(t') \right] dt' \tag{A3}$$

This leads to an expression like Eq. (A2), but with an additional exponential factor:

$$h_{mN}(t)\, h_{n1}(t+\tau)\, e^{-\varepsilon\tau} \frac{Q_0}{\varepsilon} \tag{A4}$$

This is precisely the form of Eq. (25): consequently, the effect of this term is just that shown in Fig. 3, corresponding to precursor bumps at $\omega = 0, 1, 2, \ldots$.

Summing up, we see that the net effect of these three terms is simply to renormalize the strength and broaden the δ-function spikes in the power spectrum arising from the unperturbed oscillation $\mathbf{x}_0$.

REFERENCES

1. K. Wiesenfeld, E. Knobloch, R. F. Miracky, and J. Clarke, *Phys. Rev. A* **29**:2102 (1984).
2. C. D. Jeffries and K. Wiesenfeld, *Phys. Rev. A*, to appear.
3. J. P. Crutchfield, J. D. Farmer, and B. A. Huberman, *Phys. Rep.* **92**:45 (1982).
4. J. P. Crutchfield and B. A. Huberman, *Phys. Lett.* **77A**:407 (1980).
5. J. P. Crutchfield, M. Nauenberg, and J. Rudnick, *Phys. Rev. Lett.* **46**:933 (1981).
6. B. Shraiman, C. E. Wayne, and P. C. Martin, *Phys. Rev. Lett.* **46**:935 (1981).
7. G. Meyer-Kress and H. Haken, *J. Stat. Phys.* **26**:149 (1981).
8. G. Meyer-Kress and H. Haken, *Phys. Lett.* **82A**:151 (1981).
9. J.-P. Eckmann, L. Thomas, and P. Wittwer, *J. Phys. A* **14**:3153 (1982).
10. J. E. Hirsch, B. A. Huberman, and D. Scalpino, *Phys. Rev. A* **25**:519 (1982).
11. A. B. Rechester and R. B. White, *Phys. Rev. A* **27**:1203 (1983).
12. J. Perez and C. D. Jeffries, *Phys. Rev. B* **26**:3460 (1982).
13. D. McCumber, *Phys. Rev.* **141**:306 (1966).
14. H. Haken, *Handbuch der Physik* (Encyclopedia of Physics), Vol. XXV/2C, L. Genzel, ed. (Springer, Heidelberg, 1970).
15. K. Manes and A. Siegman, *Phys. Rev. A* **4**:373 (1971).
16. J. Guckenheimer and P. J. Holmes, *Nonlinear Oscillations, Dynamical Systems and Bifurcations of Vector Fields* (Springer, New York, 1983).
17. D. W. Jordan and P. Smith, *Nonlinear Ordinary Differential Equations* (Oxford University Press, Oxford, 1977).
18. B. A. Huberman, J. P. Crutchfield, and N. H. Packard, *Appl. Phys. Lett.* **37**:750 (1980).
19. D. D'Humieres, M. R. Beasley, B. A. Huberman, and A. Libchaber, *Phys. Rev. A* **26**:3483 (1982).

20. E. Knobloch and N. O. Weiss, *Phys. Lett.* **85A**:127 (1981).
21. S. Novak and R. G. Frehlich, *Phys. Rev. A* **26**:3660 (1982).
22. J. W. Swift and K. Wiesenfeld, *Phys. Rev. Lett.* **52**:705 (1984).
23. P. Bryant and C. D. Jeffries, *Phys. Rev. Lett.* **53**:250 (1984).
24. K. Wiesenfeld, in *Fluctuations and Sensitivity in Nonequilibrium Systems*, W. Hortsthemke and D. K. Kondepudi, eds. (Springer, Berlin, 1984).
25. J. Swift, private communication.
26. W. C. Stewart, *Appl. Phys. Lett.* **12**:277 (1968).
27. E. E. McCumber, *J. Appl. Phys.* **39**:3113 (1968).
28. R. F. Miracky, J. Clarke, and R. H. Koch, *Phys. Rev. Lett.* **50**:856 (1983).
29. J. Clarke, R. F. Miracky, J. Martinis, and R. H. Koch, in *Noise in Physical Systems and 1/f Noise*, M. Savelli, G. Lecoy, and J.-P. Noufier, eds. (Elsevier Science Publishers B.V., New York, 1983).
30. R. H. Koch, R. F. Miracky, and J. Clarke, unpublished.
31. W. Horsthemke and M. Malek-Mansour, *Z. Phys.* **B24**:307 (1976).
32. W. Horsthemke and R. Lefever, *Noise-Induced Transitions* (Springer, Berlin, 1984).
33. L. Arnold, in *Fluctuations and Sensitivity in Nonequilibrium Systems*, W. Horsthemke and D. K. Kondepudi, eds. (Springer, Berlin, 1984).